Homo- and heterodinuclear arene-linked osmium(II) and ruthenium(II) organometallics: probing the impact of metal variation on reactivity and biological activity

Christopher S. Wilson, Timothy J. Prior, Jordon Sandland, Huguette Savoie, Ross W. Boyle and Benjamin S. Murray*[a]

C. S. Wilson, Dr. T. J. Prior, Dr. J. Sandland, H. Savoie, Prof. R. W. Boyle, Dr. B. S. Murray
Department of Chemistry and Biochemistry
University of Hull
Cottingham Road, HU6 7RX (UK)
E-mail: b.s.murray@hull.ac.uk

Abstract: Dinuclear metallodrugs offer much potential in the development of novel anticancer chemotherapeutics as a result of the distinct interactions possible with biomacromolecular targets and the unique biological activity that can result. Here, we describe the development of isostructural homodinuclear Os(II)-Os(II) and heterodinuclear Os(II)-Ru(II) organometallic complexes formed from the linking of the arene ligands of [M(η^6-arene)(C_2O_4)(PTA)] (M = Os/Ru; PTA = 1,3,5-triaza-7-phosphaadamantane) units. Together with the known Ru(II)-Ru(II) analogue, a chromatin-modifying agent, we probed the impact of variation of the metal ions on the structure, reactivity and biological activity of these complexes. The complexes have been structurally characterised by X-ray diffraction experiments, their stability and reactivity examined using ^{1}H and ^{31}P NMR spectroscopy and biological activity assessed, alongside mononuclear analogues, through MTT assays and cell cycle analysis (HT-29 cell line). Results revealed high antiproliferative activity in each case, with cell cycle profiles of the dinuclear complexes found to be similar to that for untreated cells, and similar but distinct profiles for the mononuclear complexes. These results indicate these complexes impact on cell viability predominantly through a non-DNA damaging mechanism of action. The new Os(II)-Os(II) and Os(II)-Ru(II) complexes reported here are further examples of a family of compounds operating via mechanisms of action atypical of the majority of metallodrugs, and which have potential as tools in chromatin research.

Introduction

Since the introduction of platinum-based chemotherapeutics for the treatment of cancer[1] there has been sustained effort toward discovering new anticancer metallodrugs of even greater efficacy and selectivity. A wide range of elements have formed the basis of these investigations, highlighted by recent examples of complexes based on Fe(II)[2], Ga(III)[3], Ag(I)[4], Re(I)[5], Os(II)[6], Ir(III)[7, 8] and Au(I)[9]. Ru(II)-based compounds have perhaps been the subject of the most intense focus, with the early compounds NAMI-A[10] and KP1019[11] then the promising RAPTA[12] and RAED[13] families of compounds paving the way for continued research in this area. Recent examples include metallodrugs which are light activated,[14] operate via catalytic mechanisms of action,[15] possess pH-dependent activity[16-18] and which target specific proteins,[19] and highlight the diverse approaches being taken.

Within the metallodrug field dinuclear metal complexes have received substantial interest in the development of novel anticancer chemotherapeutics due to the distinct biological activity they often exhibit compared to mononuclear analogues. A key feature of many dinuclear species are the unique adducts they form with biomacromolecular targets, including long range crosslinks that are not attainable by mononuclear species.

Such behaviour is seen in dinuclear (and trinuclear) platinum complexes, examples of which have been shown to form a range of long- and short-range interstrand crosslinks with duplex DNA. These adducts include the formation of 1,4-interstrand crosslinks in the 5'→5' and antiparallel 3'→3' direction that are likely to be challenging to remove by nucleotide excision repair and which induce delocalized conformational changes in DNA.[20] In line with these observations, a range of dinuclear platinum complexes, such as BBR3610 (Figure 1), have been shown to be significantly more potent than cisplatin in cell culture and animal models.[21] Interestingly, recent studies have identified proteoglycans as alternative cellular targets for di- and trinuclear platinum complexes. Through sulfate cluster anchoring these complexes were found to shield sulfated oligosaccharides from enzymatic degradation, whereas cisplatin was ineffective. Such metalloshielding behavior is of considerable potential as a strategy to inhibit the angiogenesis cascade that occurs upon the enzymatic degradation of heparan sulphate proteoglycans.[22-24] These studies further exemplify the divergent biological activity possible with di- and trinuclear platinum complexes relative to mononuclear analogues.

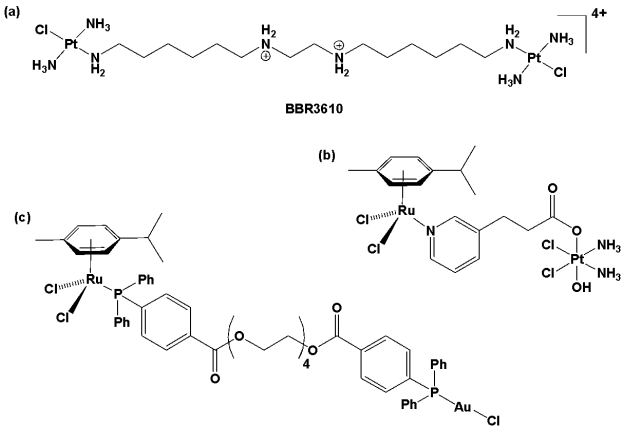

Figure 1. Examples of dinuclear metal complexes evaluated for anticancer activity: (a) the dinuclear platinum complex BBR3610, (b) a heterodinuclear ruthplatin complex highly active against cisplatin-resistant cell lines (c) a heterodinuclear Au(I)-Ru(II) complex shown to be able to crosslink a peptide through coordination to histidine residues.

Following on from these Pt(II)-Pt(II) precedents a range of dinuclear systems have been reported utilising other transition metals. An early series of half-sandwich Ru(II)-Ru(II) complexes employed bis(3-hydroxy-2-methyl-4-pyridinon-1-yl)methane-type linker groups.[25] Lipophilicity was shown to be correlated to antiproliferative activity and the complexes were shown to be able to not only crosslink two DNA duplexes but also form DNA–protein crosslinks. Recently, analogous series of Rh(III)-Rh(III) and Ir(III)-Ir(III) complexes have yielded highly cytotoxic examples able to generate reactive oxygen species and cause appreciable DNA damage at low concentrations.[26]

Au(I)-Au(I) and half-sandwich Ru(II)-Ru(II) complexes have also been reported where phosphine ligands joined via a poly(ethylene glycol) chain acted as the linking moiety. The majority of these dinuclear complexes were found to be more active than mononuclear analogues against human cancer cell lines. The antiproliferative activities of the Ru(II)-Ru(II) complexes were found to be dependent on lipophilicity whilst antiproliferative activity for the Au(I)-Au(I) series of complexes was found not to correlate to lipophilicity.[27] An analogous heterodinuclear Au(I)-Ru(II) complex (Figure 1) was later shown to crosslink a peptide through simultaneous coordination of each metal atom to different histidine residues within the peptide sequence.[28] Further heterodinuclear complexes, constructed from an Au(I)-N-heterocyclic carbene linked to (p-cymene)$RuCl_2$ or $CuCl_2$ groups via a bypyridine ligand, or to AuCl or Au-thioglucose groups via a phosphine ligand,[29] to a titanocene moiety,[30] and a (p-cymene)$RuCl_2$-Au(I)-NHC complex (RANCE-1)[31] where the metal centres are linked via bis(diphenylphosphino)methane, have also been reported. The latter compound demonstrated extremely promising inhibition of migration and invasion and angiogenesis, including effective inhibition of vascular endothelial growth factor. The linking of a Ru(II)(polypyridine) moiety, via phosphine coordination, to Au-thioglucose groups has also yielded complexes with high antiproliferative activity that exhibit negligible reactivity toward plasmid DNA,[32] whilst titanofin, a heterodinuclear compound comprised of structural fragments originating from titanocene dichloride and Auranofin, was shown to strongly inhibit invasion, migration and angiogenic assembly.[33] Ferrocene-appended half-sandwich Ir(III) complexes also yielded highly active metallodrugs, with lower IC_{50} concentrations than cisplatin against several cancer cell lines, and which inhibited migration and colony formation. Lysosome accumulation and damage resulting in apoptosis was reported.[34]

Heterodinuclear Pt(IV)-Ru(II) complexes have also been recently reported.[35] These complexes were found to be highly active towards human cancer cell lines, with typical IC_{50} values determined from monolayer MTT assays found to be in the sub-micromolar and nanomolar range. A comparison of one of the series (Figure 1) with cisplatin found the former to be more cytotoxic in a 3D multicellular spheroid model. The same Pt(IV)-Ru(II) complex was also found to inhibit cell migration in a 24 h wound healing assay – albeit at a concentration 10 fold greater than the 72 h IC_{50} value for the same cell line. Preliminary mechanistic studies highlighted the ability of the Pt(IV)-Ru(II) complex to strongly inhibit DNA replication.

A series of dinuclear Ru(II)-arene complexes has also been formed through the linking, via the arene ligands, of two [Ru(η^6-arene)Cl_2(PTA)]/[Ru(η^6-arene)(C_2O_4)(PTA)] (RAPTA) moieties.[36] The dinuclear complexes were found to exhibit significantly increased antiproliferative activity compared to mononuclear analogues toward a range of cell lines, with the nature (length, rigidity, stereochemistry) of the linking group significantly modulating biological activity. Mass spectrometric experiments confirmed the ability of the dinuclear complexes to form adducts with protein and peptide targets where each metal centre was found to coordinate to amino acid residues at different sites. In structural studies with the nucleosome core particle the dinuclear complexes were found to be able to crosslink the histone proteins H2A and H2B,[37] within a region known as the nucleosome acidic patch, through ruthenium coordination at sites which previous studies had shown were able to be occupied by mononuclear RAPTA complexes.[38] The use of rigid linkers was shown to be a route by which the sites of crosslinking could be modulated through constraining the relative localisation of each ruthenium centre. The dinuclear complexes were found to be able to efficiently generate chromatin adducts in cellulo and induce a persistent condensed state of chromatin, most likely by forming nucleosome-nucleosome crosslinks, from which the cell does not recover. Furthermore, the dinuclear complexes were found to inhibit binding of the regulator of chromosome condensation 1 (RCC1) protein to the nucleosome acidic patch. This contrasts with a mononuclear analogue which neither formed nucleosome-nucleosome crosslinks nor blocked RCC1 binding at comparable concentrations. The differences in protein crosslinking behaviour and antiproliferative activity profiles seen between dinuclear complexes and mononuclear analogues, as well as within the series of dinuclear complexes, clearly demonstrates the impact on biomacromolecular interactions of tethering two RAPTA units together, and highlights the importance of the nature of the linking moiety. Such dinuclear complexes not only have potential in the development of therapeutic agents with distinct mechanisms of action but they also hold promise in the development of tools to study the function of biomacromolecular systems. Properties such as the charge on the dinuclear complex, constraints imposed by the

linker and the nature of the metal ions may be tuned to target and crosslink specific regions on a biomacromolecule to perturb structure and dynamics and/or interfere with the binding of regulatory ligands.

Here we explore the effect on reactivity and biological activity of variation of the central metal ions within an isostructural series of homo- and heterodinuclear RAPTA-type complexes, based on Os(II)-Os(II) and Os(II)-Ru(II) combinations, along with the previously reported Ru(II)-Ru(II) analogue. Mononuclear Os(II) and Ru(II) analogues are also reported. Extensive structural data has been collected to enable comparison across the series, stability and reactivity studies of the dinuclear complexes under physiologically relevant conditions are reported and the anti-proliferative activity and the impact on the cell cycle of all complexes has been evaluated with the HT-29 cell line.

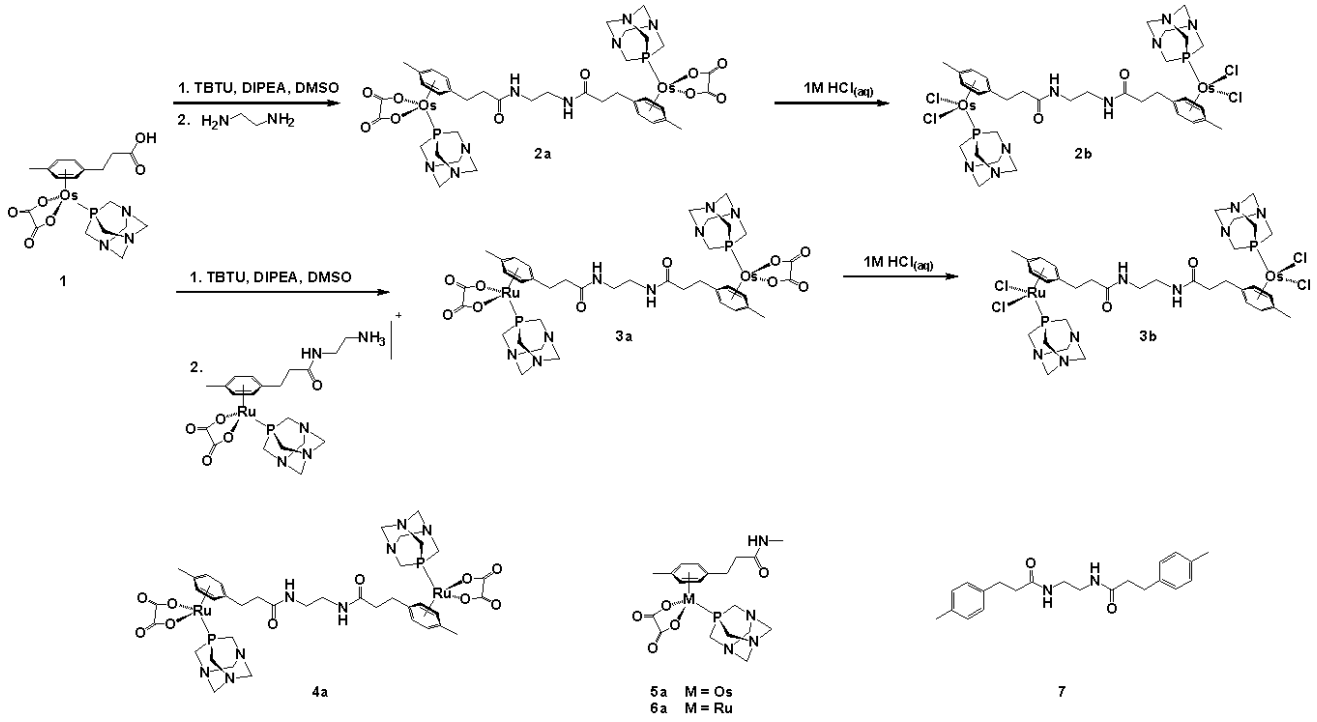

Scheme 1. Synthesis of dinuclear oxalato- and chlorido complexes .

Results and Discussion

Synthesis and characterisation

The dinuclear osmium complex, **2a**, was synthesized following methodology[36] previously applied to access the ruthenium analogue **4a** – namely via amide-forming reactions between ethylenediamine and the respective mononuclear complex, **1**, utilising the coupling agent *O*-(benzotriazol-1-yl)-*N,N,N′,N′*-tetramethyluronium tetrafluoroborate (TBTU) with *N,N*-diisopropylethylamine (DIPEA) in DMSO (Scheme 1).

An alternative synthetic route was taken to access the heterodinuclear complex, **3a**. In this case a mononuclear ruthenium complex bearing an amine group tethered to the arene ligand, **S3**, was coupled to **1** via amide-forming chemistry. This route was chosen to prevent the formation of the mixture of products that would occur if the respective mononuclear precursors **S1** and **1** were attempted to be coupled directly via ethylenediamine. The previously reported dinuclear ruthenium complex, **4a**,[36] and mononuclear osmium and ruthenium complexes **5a** and **6a** were also synthesised for this study. Full details of the synthesis of all complexes, including precursors, are given in the experimental section and ESI.

All mono- and dinuclear complexes **2a**-**6a** were isolated from their respective reaction mixtures by chromatography (silica gel, methanol/water) followed, for the dinuclear complexes, by precipitation from methanol solutions or, for the mononuclear analogues, crystallization, to yield the desired products as analytically pure yellow or orange solids. The chlorido-analogues (**2b**-**4b**) of dinuclear complexes **2a**-**4a** were obtained by dissolution of the oxalato-complexes in $HCl_{(aq)}$ (1 M) and stirring at room temperature for 72 h, followed by precipitation of the target complexes as their HCl salts with 2-propanol then subsequent lyophilization of a $HCl_{(aq)}$ solution of the complex. All complexes are water soluble and were characterised by ^{1}H, ^{31}P, ^{13}C NMR, elemental analysis and high-resolution mass spectrometry.

Within the NMR spectra of the heterodinuclear complex **3a** the presence of both the half-sandwich Os(II) and Ru(II) components is clearly indicated through distinct sets of signals observed for the arene and PTA ligands coordinated to each metal. In the ^{1}H NMR spectrum this is exemplified by the presence of Os-arene signals in the region 6.06-6.11 ppm compared to Ru-arene signals in the region 5.91-5.96 ppm, and in the ^{31}P NMR spectrum the PTA phosphorus signals appear at -66.7 ppm (Os-P) and -32.8 ppm (Ru-P). When compared to the NMR spectra for the homodinuclear complexes **2a** and **4a** the spectra of **3a** are clearly

comprised of elements from both. High-resolution mass spectrometry further confirms the constitution of each dinuclear species, with the isotopic distributions observed within each spectrum reflecting the differing metal compositions of each dinuclear complex (Figures S32-35).

Structural commentary

The molecular structures of **2a**-**6a**, as well as the precursors $[M(\eta^6\text{-ethyl 3-}(p\text{-tolyl})\text{propanoate})Cl_2]_2$ and $[M(\eta^6\text{-3-}(p\text{-tolyl})\text{propanoic acid})Cl_2]_2$ (M = Ru, Os) were confirmed by single crystal X-ray diffraction data obtained from crystals grown by vapour diffusion of acetone into water/acetone solutions of the complexes, or diffusion of diethyl ether into methanol solutions of the complexes (Figures 2-3, S1-S7, Tables S1-S3). The data confirms the structural similarity across the series of dinuclear complexes where **2a**, **3a**, and **4a** are isostructural and as such only the structure of **3a** is described. **3a** crystallises in the centric space group $P2_1/c$ with a single metal ion in the asymmetric unit (Figure 2). The extended dimer is generated by the symmetry operation $-x, 2-y, 2-z$. There is small scale disorder of the linking ethylene group (C11a/C11b) as this can adopt two different orientations and this was dealt with using standard procedures. Each of the structures crystallises with water present. The water resides in channels that run parallel to the crystallographic *c* direction. There is some small variation of the amount of water present in the three compounds.

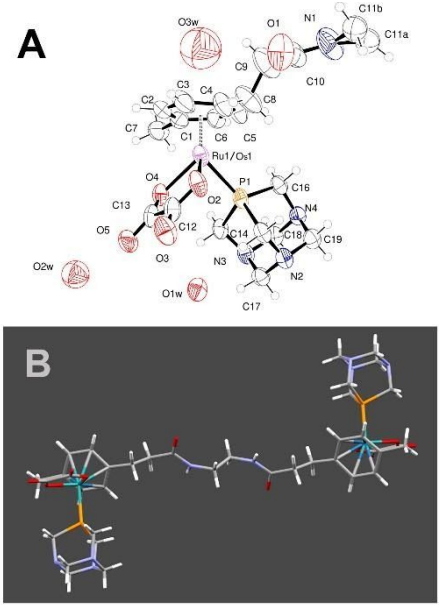

Figure 2. (A) Asymmetric unit of **3a** with atoms shown as 50% probability ellipsoids; (B) Dinuclear complex in **3a** generated by the centre of inversion.

For **2a** and **4a** only one type of metal ion is present but for **3a** the two ends of the extended dimer are expected from the synthesis to have different metal ions. A structure refinement to demonstrate the presence of both metals in the dimer was carried out in this way. Initially the structure was refined using 100 % Ru but the fit was rather poor (wR2 = 0.2768). When 50 % Ru and 50 % Os were used in the model there was a huge improvement in the quality of the fit (wR2 = 0.2245). These occupancies were fixed at 0.5 and 0.5. It is possible to carry out a free refinement of the metal site but this converges near to 50:50 and there is little improvement in the quality of fit to F^2.

Likewise, **5a** and **6a** are isostructural and each crystallises in the centric space group Pwith a single molecule in the asymmetric unit. The Os example will be discussed as representative of the two structures. The metal ion is coordinated by the arene, a single PTA ligand bound through phosphorus, and by bidentate oxalate (as shown in Figure 3). The amide functionality (N1-H1) forms a short hydrogen bond to an oxalate of an adjacent molecule: N1-H1 0.96 Å; N1···O6^i 2.897(15) Å; N-H···O6^i 166 ° (where symmetry equivalent atom is generated by $i = x, y-1, z$). There is a longer contact to O4^i for which N1···O4^i is 3.205(16) Å and N1-H1…O4^i is 120 °. These interactions form a hydrogen-bonded chain that extends parallel to the crystallographic *b* direction.

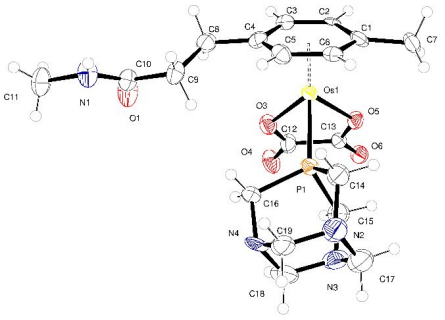

Figure 3. Asymmetric unit of **5a** with atoms shown as 50% probability ellipsoids.

Stability studies and reactivity

The stability of the dinuclear compounds **2a**-**4a** was compared in D_2O (0.1 M NaCl) and in McCoys 5A Medium (Modified) (supplemented with 10% Fetal Calf Serum (FCS)), with incubations performed at 310 K for 72 h. In saline solution all complexes showed minor changes over 72 h as seen in the appearance of new, minor Ru/Os(II)-η^6-arene signals (^{1}H NMR) and phosphorus signals (^{31}P NMR) indicative of some ligand exchange at ruthenium and osmium centres (Figures S23-S26). However, for complexes **3a** and **4a** there were also minor levels of dissociated arene ligand after 72 h that indicated the increased lability of the Ru(II)-η^6-arene group relative to the Os(II)-η^6-arene group, as no dissociated arene ligand was observed with **2a** over 72 h. In McCoys 5A Medium (Modified) (supplemented with 10% FCS) new phosphorus signals (^{31}P NMR) associated with the Os-PTA (**2a**, **3a**) and Ru-PTA (**3a**, **4a**) groups were present after 72 h incubation indicative of a change in coordination environment at the metal centres (Figures S27-S29). Similar changes have been previously observed with an analogous mononuclear oxalate-complex in Dulbecco's Modified Eagle Medium (DMEM) and RPMI 1640 medium and were attributed to the exchange of the oxalato ligand.[36] Such exchange provides a route by which **2a**-**6a**, in which the metal centres are protected by the bidentate oxalato-ligand, may be 'activated' by their transformation into more active species.

The reactivity of the chlorido complexes **2b**-**4b**, utilized as non-protected models of **2a**-**4a**, towards potential intracellular ligands was assessed by their incubation with 6 eq. guanosine 5′-monophosphate (5′-GMP) (72 h, 310 K, 5 mM NaCl, pD 7.4 150 mM phosphate buffer). In each case extensive reaction of the complexes with 5′-GMP was observed (^{1}H NMR) as indicated by the change in the form of the spectra over 72 h in the η^6-arene region, and the appearance of multiple new 5′-GMP H8 signals (Figures S30-S31), indicative of the metal ion coordinating to the N7 of 5′-GMP. Spectra are invariably complex due to the range of potential adducts (including diastereoisomeric adducts) that may form under these conditions but clearly indicate the potential of both metal centres to participate in reactivity as determined in previous studies with **4b**.[36, 37]

Evaluation of *in vitro* anticancer activity

Earlier studies highlighted the increased antiproliferative activity of **4a** against the A2780, A2780-cisR and HEK-293 cell lines relative to a mononuclear analogue.[36] Additionally, differences were observed in the cell cycle profile of HeLa cells treated with **4b** compared to the mononuclear analogue RAPTA-C,[37] with the latter perturbing the proportion of cells distributed between the G0/G1, S and G2/M phases whilst treatment with **4b** resulted in a cell cycle profile that was statistically identical to that of untreated cells.

The antiproliferative profile of the new compounds **2a**,**3a**,**5a** and **6a**, as well as **4a**, was evaluated in the HT-29 cell line using the MTT assay. The oxalato compounds were chosen to be assessed rather than their chlorido analogues due to their relative ease of synthesis and purification, whilst previous studies have shown the potency of related oxalato complexes to mirror that of their chlorido analogues.[36] Antiproliferative activity was found to be similar across the series of dinuclear compounds in the order **4a** > **3a** > **2a** (Table 1). For **4a** the IC_{50} of 1.3 ± 0.1 μM is at least 17-times lower than that previously observed against the A2780, A2780cisR and HEK-293 cell lines.[36] The antiproliferative activity of the arene ligand **7** was also recorded and found to be >500 μM indicating that the antiproliferative activity observed with **2a**-**4a** is not ligand based. The mononuclear compounds **5a** and **6a** were also found to be active toward the HT-29 cell line, with IC_{50} concentrations of 6.3 ± 3.1 μM and 3.9 ± 0.6 μM respectively. These results indicate that **4a** is more active than its mononuclear analogue **6a** with respect to the total metal dose administered, whilst **2a** and **5a** are equally active based on the total metal dose administered. All complexes were significantly more active than cisplatin (IC_{50} > 50 μM) against the HT-29 cell line.

Table 1. In vitro antiproliferative activity of **2a**-**6a**, arene ligand **7** (*N*,*N*'-(ethane-1,2-diyl)bis(3-(*p*-tolyl)propanamide)), and cisplatin toward the human colorectal adenocarcinoma (HT-29) cell line following 72 h exposure (data represents the mean value ± standard deviation, n=3).

Compound	IC_{50} (μM)
2a	2.8 ± 0.4
3a	1.6 ± 0.1
4a	1.3 ± 0.1
5a	6.3 ± 3.1
6a	3.9 ± 0.6
Arene ligand 7	>500
Cisplatin	>50

Cell cycle analysis was performed to assess the overall impact of treatment with the mono- and dinuclear compounds and, as DNA adduct formation was found not to be significant with **4b** in earlier studies,[37] to assess the degree of DNA adduct formation by the complexes. Cells were treated with the complexes for 48 h at their 72 h IC_{50} concentrations to standardize the extent of damage induced by the series of compounds tested. The cell cycle profiles obtained with dinuclear and mononuclear complexes are very similar to that of the untreated cells (Figure 4). The mononuclear complexes **5a** and **6a** resulted in low increases in the proportion of cells in the G0/G1-phase whilst **3a** resulted in a marginal increase in cells in the G2/M phase. The similarity of the cell cycle profiles obtained with **2a**-**4a** and that of the untreated cells, with no arrest of the cell cycle at the S or G2/M phases, indicates that none of these complexes yield significant levels of DNA adducts. These results align with those previously reported,[37] where treatment of HeLa cells with analogous dinuclear complexes yielded cell cycle profiles identical to untreated cells. The cell cycle profiles obtained with mononuclear complexes **5a** and **6a** are similar but distinct from those of **2a**-**4a** and are dramatically different to that previously reported[37] for the analogues mononuclear complex RAPTA-C (increased cell proportions in S and G2/M phases, reported with the HeLa cell line, and linked to earlier observations of RAPTA-C DNA binding). **5a** and **6a** are likely to exert their biological activity without significant formation of DNA adducts, although based on the cell cycle profiles these are likely to be more significant that for **2a**-**4a**. Flow cytometry also revealed an increase in the proportion of non-viable cells for samples treated with complexes **2a**-**6a** compared to untreated cells (Figure S10). This observation is consistent with an increase in cells with reduced DNA content, potentially as a consequence of apoptosis and loss of DNA fragments during sample preparation, and is consistent with the antiproliferative activity of **2a**-**6a**.

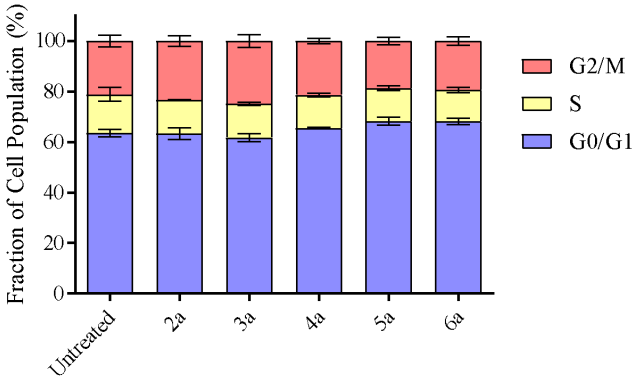

Figure 4. Cell cycle analysis of HT-29 cells treated with **2a**-**6a**. Cell cycle analysis was performed by flow cytometry (data represents the mean value ± standard deviation, n=3).

Conclusions

Synthetic routes to access the homodinuclear Os(II)-Os(II) complexes, **2a** and **2b**, and the heterodinuclear Os(II)-Ru(II) complexes, **3a** and **3b**, have been established and the impact of the variation of the metal ions within these complexes on their stability, reactivity

and biological activity has been assessed, in conjunction with comparisons to the known Ru(II)-Ru(II) complexes **4a** and **4b**. The antiproliferative activity of the dinuclear complexes **2a**-**4a** was found to be of a similar level across the series and parallels the similar levels of reactivity (**2b**-**4b**) and activation (by oxalato exchange) (**2a**-**4a**) observed for these complexes. The highly antiproliferative nature of these complexes likely stems from their ability to form adducts with biomacromolecular targets in cellulo, as previously established with **4b**, and indicates that modulating the central metal ions from Ru(II) to Os(II) does not impede complex activation in cell culture conditions, e.g. via oxalato exchange. The increased stability observed with the Os(II)-η^6-arene moieties within these complexes relative to the Ru(II)-η^6-arene moieties can be rationalized in terms of the expected increase in metal-arene binding energies on going from Ru(II)-η^6-arene to Os(II)-η^6-arene.[39] The high antiproliferative activity also exhibited by the mononuclear complexes **5a** and **6a**, although not as potent as the most active dinuclear complex **4a**, indicates the ability of these compounds to also form damaging adducts, such as metalation of histone proteins, in cellulo.

Cell cycle analysis revealed at most only a minor impact of complexes **2a**-**6a** on specific cell cycle phases relative to untreated cells, for **2a**-**4a** this mirrors previous observations with **4b** and HeLa cells, but for the mononuclear complexes, **5a**-**6a**, this contrasts with results seen with RAPTA-C which did significantly impact the cell cycle phase distribution of HeLa cells.[37] Given that substantial DNA adduct formation with these complexes would be expected to impact on cell cycle profile, the antiproliferative activity observed is likely exerted without the formation of substantial levels of DNA adducts, although further experiments would be required to confirm this. Clearly the cellular impact of **2a**-**6a** bears close resemblance to that of the recently reported dinuclear Ru(II)-Ru(II) complexes[36, 37] that are chromatin-modifying agents and it is likely that chromatin interactions are important to the action of **2a**-**6a**. Further experiments are required to probe any differences in the nature of any such adducts formed with these dinuclear and mononuclear complexes.

Overall, the new synthetic routes described here allow the development of stable dinuclear Os(II)-Os(II) complexes that may find utility in chromatin research through the formation of persistently crosslinked adducts. They also allow for the possible development of novel dinuclear organometallic structures where each metal-containing component has been designed to interact with different classes of biomacromolecular targets e.g. protein and DNA targeting. Work is ongoing in these areas.

Experimental Section

Materials

All commercially purchased materials were used as received. Osmium(III) chloride hydrate was purchased from Acros organics. 3-(*p*-tolyl)propionic acid was purchased from Alfa Aesar. Ammonia was purchased from Energas. Dimethylsulfoxide-d_6 and deuterium oxide were purchased from Eurisotop. 4-Methylcinnamic acid (predominantly trans), lithium, HCl (37 %), *N,N*-diisopropylethylamine (DIPEA), *N,N*-dimethylformamide (DMF), silver nitrate, sodium oxalate and sodium sulfate were purchased from Fisher Scientific. Guanosine 5′-monophosphate disodium salt, ruthenium(III) chloride hydrate, *O*-(benzotriazol-1-yl)-*N,N,N′,N′*-tetramethyluronium tetrafluoroborate (TBTU), di-*tert*-butyl dicarbonate, ethylenediamine and silica gel (60Å 40-63 micron) were purchased from Fluorochem Ltd. Acetone, ethanol, ethyl acetate, dichloromethane (DCM), dimethyl sulfoxide (DMSO), methanol and 2-propanol were purchased from Honeywell. Methylamine hydrochloride, 3-(*p*-tolyl)propanoic acid and 1,3,5-triaza-7-phosphaadamantane (PTA) were purchased from Sigma Aldrich. Diethyl ether was purchased from VWR.

Instrumentation and Methods

NMR

^{1}H, ^{13}C and ^{31}P NMR spectra were recorded on a Jeol JEOL ECZ 400S spectrometer (^{1}H at 400.2 MHz, ^{13}C at 100.6 MHz and ^{31}P at 162.0 MHz). Spectra are referenced internally to residual solvent peaks (D_2O: ^{1}H δ 4.79 ppm, ^{13}C δ unreferenced; DMSO-d_6: ^{1}H δ 2.50 ppm, ^{13}C δ 39.52 ppm); ^{31}P NMR spectra are reported relative to an external 85% H_3PO_4 reference (δ 0 ppm). Spectra were acquired at 295 K unless stated otherwise.

Mass spectrometry

Accurate mass measurements were performed at the University of Hull using a Bruker Maxis Impact QqTOF MSMS. Before mass measurement the instrument was calibrated against sodium formate over the range 90 to 1550 Da. Resolution used was typically 45000. Samples (as solutions in methanol, 10^{-5} M) were injected into a solvent stream from a syringe pump at 3 µl min^{-1} via a 5 µl loop injector. The data was then internally mass measured against an internal calibrant peak from hexakis(1H,1H,4H-hexafluorobutyloxy)phosphazine (CAS No. 186406-47-2) $C_{24}H_{18}O_6N_3P_3F_{36}$ *m/z* 1220.99064. An average result from 3-5 separate injections is quoted. The mass was measured and calculated using Bruker DataAnalysis 4.2 software.

Crystal structure determinations

Experimental X-ray single crystal diffraction data were collected using various instruments. Data for **[Os(η^6-3-(p-tolyl)propanoic acid)Cl$_2$(PTA)]**, **5a**, **[Os(η^6-ethyl 3-(*p*-tolyl)propanoate)Cl$_2$]$_2$**, **[Ru(η^6-ethyl 3-(*p*-tolyl)propanoate)Cl$_2$]$_2$**, **[Os(η^6-3-(*p*-tolyl)propanoic acid)Cl$_2$]$_2$** and **[Ru(η^6-3-(*p*-tolyl)propanoic acid)Cl$_2$]$_2$** were collected using a Stoe IPDS2 image plate diffractometer operating with Mo radiation. Data for **2a**, **3a**, **4a**, and **6a** were collected by the EPSRC National Crystallography Service (NCS), Southampton, UK, using either Cu or Mo radiation. **[Os(η^6-methyl 3-(*p*-tolyl)propanoate)Cl$_2$(PTA)]** was studied by the NCS using synchrotron radiation at Station I19 of the Diamond Light Source, UK. In each case data were treated for the effects of absorption.

Crystal structures were solved using dual space methods implemented within SHELXT[40] and refined using SHELXL-2018/3.[41] Non-hydrogen atoms were located using difference Fourier methods and refined using anisotropic displacement parameters. Hydrogen atoms were placed at geometrically calculated positions using a riding model. CCDC 1945446-1945450 and 1945456-1945462 contain the supplementary crystallographic data for this paper. These data can be obtained free of charge via www.ccdc.cam.ac.uk/data_request/cif.

Elemental Analysis

Elemental analysis was performed at the University of Hull. Analysis was performed with the addition of V_2O_5 to samples.

Synthesis

[Ru(η^6-3-(*p*-tolyl)propanoic acid)PTA(C_2O_4)] (**S1**)[36], silver oxalate[42] and *tert*-butyl (2-aminoethyl)carbamate[43] were prepared according to literature procedures. Complex **6a** was prepared as described by Sandland et al.[44]

3-(4-methylcyclohexa-1,4-dien-1-yl)propanoic acid: 4-Methylcinnamic acid (predominantly trans) (21.54 g, 132.8 mmol) was added to a solution of NH_3 (1 L) and EtOH (100 ml) cooled at -78°C, followed by further EtOH (100 ml). The resulting colourless solution was stirred with a mechanical stirrer followed by the addition of lithium (8.51 g, 1.23 mol) piecewise (approx. 200 mg of lithium per addition then waiting until this had been consumed before the subsequent addition) to result in a viscous precipitate. After the final addition of lithium the blue colour persisted for several minutes before fading to leave a white suspension – the reaction mixture was left to warm to room temperature for 18 h. The resulting white solid was suspended in H_2O (200 ml) and cooled on ice – the pH was then adjusted to 1 with concentrated $HCl_{(aq)}$ and the resulting white suspension was extracted with DCM (3 x 100 ml). The combined organic phases were washed with H_2O (100 ml), dried with Na_2SO_4, filtered then dried under reduced pressure to leave a mixture of 3-(4-methylcyclohexa-1,4-dien-1-yl)propanoic acid and 3-(*p*-tolyl)propionic acid (1:1.06) as a white solid (21.2 g (10.2 g product, 62.1 mmol, 47 %)). Analytical data for the product 3-(4-methylcyclohexa-1,4-dien-1-yl)propanoic acid concurred with that previously reported.[45]

[Os(η⁶-ethyl 3-(*p*-tolyl)propanoate)Cl₂]₂: To a mixture of 3-(4-methylcyclohexa-1,4-dien-1-yl)propanoic acid (1.68 g, 10.11 mmol) and 3-(*p*-tolyl)propionic acid (1.76 g, 10.72 mmol) was added $OsCl_3.xH_2O$ (1 g, 3.37 mmol, anhydrous basis) followed by ethanol (12 ml). The dark suspension was heated and maintained at reflux for 3 h then the resulting orange/brown light suspension was filtered whilst hot, the solid washed with further ethanol (50 ml) then the combined filtrates were left to stand in the fridge. After 18 h crystals had formed - the solvent was decanted and the crystals washed with ethanol (5 ml) then diethyl ether (20 ml). The crystals were collected and dried under reduced pressure to yield the desired product as a crystalline red solid (503 mg, 0.555 mmol, 33 %). The remaining filtrate was concentrated to a volume of 20 ml then left to stand in the fridge. After 18 h a further crop of crystals had formed and were washed with ethanol (5 ml), diethyl ether (20 ml) then dried under reduced pressure to yield further product as a red crystalline solid (210 mg, 0.232 mmol, 14 %). A sample of the product was heated at 100°C under reduced pressure to remove residual ethanol for characterisation purposes. ^{1}H NMR (DMSO-d_6, 400 MHz): δ = 6.10 (d, 4H, *J* = 5.5 Hz, 4 x Ar C*H*), 6.00 (d, 4H, *J* = 6 Hz, 4 x Ar C*H*), 4.06 (q, 4H, *J* = 7.0 Hz, 2 x -CH_2-CH$_3$), 2.63 (m, 8H, 2 x -CH_2-CH_2-), 2.11 (s, 6H, 2 x ArCH_3), 1.17 (t, 6H, *J* = 7.0 Hz, 2 x –CH$_2$CH_3); ^{13}C{^{1}H} NMR (DMSO-d_6, 100 MHz): δ = 172.1, 93.1, 90.2, 80.4, 77.9, 60.1, 33.3, 27.1, 17.8, 14.2; $C_{24}H_{32}Cl_4O_4Os_2$ (%): calcd C 31.79 H 3.56 found C 32.07 H 3.47.

[Os(η⁶-3-(*p*-tolyl)propanoic acid)Cl₂]₂: A suspension of [Os(η^6-ethyl 3-(*p*-tolyl)propanoate)Cl$_2$]$_2$ (298 mg, 0.329 mmol) in $HCl_{(aq)}$ (4 ml, 0.05 M) was stirred for 6h at 20°C then diluted with $HCl_{(aq)}$ (15 ml, 1 M) and left to stir for a further 48 h at 20°C at which point NMR analysis of a dried aliquot indicated hydrolysis had proceeded to completion. The reaction mixture was filtered through a Millex LG 0.20 µm PTFE syringe filter then evaporated to dryness under reduced pressure at 40°C. The desired product was isolated as a yellow powder in quantitative yield. ^{1}H NMR (DMSO-d_6, 400 MHz): δ = 6.09 (d, 4H, *J* = 5.0 Hz, 4 x Ar C*H*), 6.00 (d, 4H, *J* = 5.0 Hz, 4 x Ar C*H*), 2.58 (s, 8H, 2 x -CH_2-CH_2-), 2.12 (s, 6H, 2 x ArCH_3); ^{13}C{^{1}H} NMR (DMSO-d_6, 400 MHz): δ = 173.7, 92.8, 90.7, 80.3, 78.0, 33.5, 27.2, 17.7; $C_{20}H_{24}Cl_4O_4Os_2$(%): calcd C 28.24 H 2.84 found C 28.13 H 2.54.

Complex 1: To a suspension of [Os(η^6-3-(*p*-tolyl)propanoic acid)Cl$_2$]$_2$ (281 mg, 0.33 mmol) in H_2O (10 ml) was added silver oxalate (370 mg, 1.22 mmol) and the mixture was stirred in the dark for 18 h. The suspension was then allowed to settle and the liquid filtered through a Millex LG 0.20 µm PTFE syringe filter then through a pipette plugged with cotton wool. Water was removed under reduced pressure at 45°C then the residue dried under high vacuum to yield a yellow/green glassy solid (239 mg). PTA (82 mg, 0.522 mmol) was then added to the solid followed by MeOH (20 ml) – the mixture was briefly sonicated to detach all solid from the glassware then left to stir. After 18 h the resultant suspension was allowed to settle, the solvent was decanted and the solid then dried under reduced pressure at 40°C. The residue was then dissolved in H_2O then lyophilized to yield the product as a yellow powder (259 mg, 0.432 mmol, 83 % from PTA (65 % from the starting dimer)). ^{1}H NMR (D$_2$O, 400 MHz): δ = 6.14 (d, 2H, *J* = 6.0 Hz, 2 x Ar C*H*), 6.03 (d, 2H, *J* = 5.0 Hz, 2 x Ar C*H*), 4.59 (m, 6H, PTA), 4.12 (s, 6H, PTA), 2.63 (m, 4H, -CH_2-CH_2-), 2.13 (m, 3H, ArCH_3); ^{31}P{^{1}H} NMR (D$_2$O, 162 MHz): δ = -64.8; ^{13}C{^{1}H} NMR (D$_2$O, 100 MHz): δ = 177.4, 166.1, 90.7, 88.1, 81.3 (d, *J* = 3.0 Hz), 80.0 (d, *J* = 4.0 Hz), 70.6 (d, *J* = 7.0 Hz), 47.3 (d, *J* = 21.0 Hz), 34.9, 27.8, 17.4; HRMS (ES$^+$) *m*/*z* found 602.1108 [M + H]$^+$ $C_{18}H_{15}N_3OsP$ requires 602.1091; $C_{18}H_{24}N_3O_6OsP$ (%): calcd C 36.06 H 4.03 N 7.01 found C 35.82 H 4.05 N 6.91.

Complex 2a: A suspension of [Os(η^6-3-(*p*-tolyl)propanoic acid)PTA(C$_2$O$_4$)] (**1**) (0.1 g, 0.167 mmol) and TBTU (54 mg, 0.168 mmol) in DMSO (4 ml) was stirred for 1 min followed by the addition of DIPEA (145 µl, 0.832 mmol) – over 5 min the mixture solubilised then ethylenediamine (5.6 µl, 0.084 mmol) was added and the reaction mixture was left to stir. After 1 h TLC analysis (50:50 MeOH:H_2O, silica gel) indicated all starting reagents had been consumed; the reaction mixture was added to a silica gel column (4 cm x 10 cm loaded in acetone) with acetone (15 ml) in excess in the solvent reservoir. The solvent was eluted to allow the yellow suspension to settle onto the silica gel. The column was then eluted with acetone (400 ml to remove DMSO), MeOH (500 ml) then MeOH + H_2O (10% -> 30%) (1 L). The combined product fractions were combined and concentrated to a volume of 6 ml under reduced pressure at 60°C then lyophilised to yield a yellow powder. The solid was then dissolved in H_2O (2 ml) and diluted with acetone until precipitation commenced. The mixture was left to vapour diffuse in acetone and after 48 h crystals had formed that were harvested, washed with acetone then dried under reduced pressure. The dried crystalline solid was dissolved in MeOH (2 ml) and on standing a solid precipitated which was then collected by centrifugation, washed with MeOH (1 ml) then collected by centrifugation. The solid was then dissolved in H_2O and dried at 55°C under reduced pressure to remove residual MeOH – the residue was then dissolved in H_2O and lyophilized to leave the desired product as a yellow powder (15 mg, 0.012 mmol, 14 %). ^{1}H NMR (D$_2$O, 400 MHz): δ = 6.06 (d, 4H, *J* = 5.5 Hz, 4 x Ar C*H*), 6.02 (d, 4H, *J* = 6.0 Hz, 4 x Ar C*H*), 4.50 (m, 12H, PTA), 4.08 (s, 12H, PTA), 3.20 (s, 4H, -HN-CH_2-CH_2-NH-), 2.55 (m, 8H, -CH_2-CH_2-), 2.13 (m, 6H, ArCH_3); ^{31}P{^{1}H} NMR (D$_2$O, 162 MHz): δ = -66.7; ^{13}C{^{1}H} NMR (D$_2$O, 100 MHz): δ = 174.5, 166.0, 90.1, 87.7, 80.8 (d, *J* = 4.0 Hz), 79.9 (d, *J* = 4.0 Hz), 70.5 (d, *J* = 7.5 Hz), 47.6 (d, *J* = 21.0 Hz), 38.5, 36.1, 28.6, 17.4; HRMS (ES$^+$) *m*/*z* found 613.1328 [M + 2H]$^{2+}$ $C_{38}H_{54}N_8O_{10}Os_2P_2$ requires 613.1317; $C_{38}H_{52}N_8O_{10}P_2Os_2.3H_2O$ (%): calcd C 35.73 H 4.58 N 8.77 found C 35.66 H 4.42 N 8.78.

Complex 2b: **2a** (33 mg, 0.025 mmol based on **2a** obtained as its trihydrate) was dissolved in $HCl_{(aq)}$ (1M, 0.1 ml). The solution remained yellow coloured throughout the reaction – it was left to stand at room temperature for 72 h. The product was then precipitated by the addition of 2-propanol and the solid collected by centrifugation – the solid was redissolved in $HCl_{(aq)}$ (1M, 0.1 ml) and precipitated by the addition of 2-propanol. The solution was collected by centrifugation, redissolved in $HCl_{(aq)}$ then lyophilized to yield the product as a yellow solid (19 mg). ^{1}H NMR (DMSO-d_6, 400 MHz): δ = 8.06 (s, 2H, 2 x N*H*), 6.02 (d, 4H, *J* = 6.0 Hz, 4 x Ar C*H*) 5.94 (d, 4H, *J* = 6.0 Hz, 4 x Ar C*H*), 4.82 (m br, 12H, PTA), 4.24 (m, 12H, PTA), 3.06 (s, 4H, -HN-CH_2-CH_2-NH-), 2.40 (m, 8H, -CH_2-CH_2-), 2.04 (s, 6H, ArCH_3); ^{31}P{^{1}H} NMR (DMSO-d_6, 162 MHz): δ = -68.6; HRMS (ES$^+$) *m*/*z* found 1191.1699 [M + H]$^+$ $C_{34}H_{53}Cl_4N_8O_2Os_2P_2$ requires 1191.1692.

Complex S2: [Ru(η^6-3-(*p*-tolyl)propanoic acid)PTA(C$_2$O$_4$)] (**S1**) (0.1 g, 0.196 mmol) and TBTU (0.069 g, 0.215 mmol) were suspended in DMSO (1 ml) followed by the addition of DIPEA (171 µl, 0.982 mmol). The suspension was allowed to stir for 5 min followed by the addition of *tert*-butyl (2-aminoethyl)carbamate (32 mg, 0.200 mmol) as a solution in DMSO (1 ml). After stirring for 1 h further TBTU (0.069 g, 0.215 mmol) and DIPEA (34 µl, 0.195 mmol) was added and the reaction allowed to stir for a further 1 h. The reaction mixture was then added to a silica gel column (3 cm x 10 cm loaded in acetone) with acetone (20 ml) in excess in the solvent reservoir. The solvent was eluted to allow the yellow suspension to settle onto the silica gel. The column was then eluted with methanol until a yellow band eluted. The yellow solution was dried under reduced pressure, resuspended in MeOH (0.5 ml), diluted with acetone (10 ml) then the solid removed by centrifugation. The solvent was filtered through a Millex LG 0.20 µm PTFE syringe filter then dried under reduced pressure. The residue was dissolved in H_2O (0.5 ml) and diluted with MeOH (0.5 ml) then loaded onto a silica gel column (3 cm x 10 cm loaded in MeOH/H_2O - 50:50) and eluted with MeOH/H_2O - 50:50. The desired product eluted over 30 ml (R_f = 14/29, MeOH/H_2O - 50:50) – the solution was dried under reduced pressure at 45°C to leave the desired product as a glassy yellow solid (0.087 g, 0.133 mmol, 68 %). ^{1}H NMR (D$_2$O, 400 MHz): δ = 5.89 (m, 4H, 4 x Ar C*H*), 4.53 (s, 6H, PTA), 4.12 (s, 6H, PTA), 3.08-3.21 (m, 4H, -NH-CH_2-CH_2-NH-), 2.55 (s, 4H, -CH_2-CH_2-), 2.02 (s, 3H, ArCH_3), 9.50 (s, 9H, ^{t}Bu CH_3); ^{31}P{^{1}H} NMR (D$_2$O, 162 MHz): δ = -32.8; ^{13}C{^{1}H} NMR (D$_2$O, 100 MHz): δ = 174.2, 166.0, 158.2, 98.3, 96.7, 88.3, 87.8, 80.9, 70.6 (d, *J* = 6.5 Hz), 48.5 (d, *J* = 15.5 Hz), 39.2, 39.1, 35.5, 28.1, 27.6, 17.3; HRMS (ES$^+$) *m*/*z* found 654.1649 [M + H]$^+$ $C_{25}H_{39}N_5O_7PRu$ requires 654.1632.

Complex S3: [Ru(η^6-*tert*-butyl (2-(3-(p-tolyl)propanamido)ethyl)carbamate)PTA(C_2O_4)] (0.084 g, 0.129 mmol) was dissolved in $HCl_{(aq)}$ (1M, 4 ml) to form a red solution that was stirred for 18 h then dried under reduced pressure at 60°C to leave a red oil. Silver oxalate (0.117 g, 0.385 mmol) was added to the reaction flask and the mixture suspended in H_2O (10 ml) then left to stir in the dark for 2 h – ^{1}H NMR analysis indicated the reaction had not proceeded to completion so further silver oxalate (0.048 g, 0.158 mmol) was added to the reaction mixture. The mixture was stirred for 18 h followed by isolation of the liquid component by centrifugation then dried under reduced pressure at 60°C to leave crude product as an orange solid in quantitative yield. HRMS (ES$^+$) *m*/*z* found 554.1109 $[M + H]^+$ $C_{20}H_{31}N_5O_5PRu$ requires 554.1106.

Complex 3a: **1** (0.047 g, 0.078 mmol) and TBTU (0.025 g, 0.078 mmol) were suspended in DMSO (0.5 ml) followed by the addition of DIPEA (68 µl, 0.390 mmol). The reaction mixture was stirred for 5 min, during which it solubilised, followed by the addition of **S3** as its mixed oxalic acid salt (47 mg, 0.078 mmol) as a solution in DMSO (0.7 ml). The reaction mixture was stirred for 1 h then added to acetone (12 ml) to form a suspension that was added to a silica gel column (5 cm x 8 cm loaded in acetone) with acetone (20 ml) in excess in the solvent reservoir. The solvent was eluted to allow the yellow suspension to settle onto the silica gel. The column was then eluted with acetone (200 ml) then methanol (400 ml) until a yellow band eluted. The product was then eluted with H_2O:MeOH (50:50) and collected over a volume of 250 ml of eluted solvent. The yellow solution was dried under reduced pressure at 55°C. The product was dissolved in H_2O (0.7 ml) and the solution diluted with acetone (4 ml) – the solution was then left to vapour diffuse with acetone to yield crystalline material over 48 h that was harvested, dissolved in H_2O then lyophilized to yield the product as a dark orange solid (16 mg, 0.014 mmol, 18 %). ^{1}H NMR (D_2O, 400 MHz): δ = 6.11 (d, 2H, *J* = 5.0 Hz, 2 x Ar C*H*), 6.06 (d, 2H, *J* = 5.5 Hz, 2 x Ar C*H*), 5.95 (d, 2H, *J* = 6.5 Hz, 2 x Ar C*H*), 5.92 (d, 2H, *J* = 6.0 Hz, 2 x Ar C*H*), 4.50-4.60 (m, 12H, PTA), 4.16 (s, 6H, PTA), 4.12 (s, 6H, PTA), 3.24 (s, 4H, -HN-CH_2-CH_2-NH-), 2.53-2.65 (m, 8H, -CH_2-CH_2-), 2.17 (s, 3H, ArCH_3), 2.06 (s, 3H, ArCH_3); ^{31}P{^{1}H} NMR (D_2O, 162 MHz): δ = -32.8, -66.7; ^{13}C{^{1}H} NMR (D_2O, 100 MHz): δ = 174.5, 174.2, 166.1, 98.3, 96.9, 90.2, 88.3 (d, *J* = 3.0 Hz), 87.9, 87.8 (d, *J* = 4.0 Hz), 80.8 (d, *J* = 4.0 Hz), 80.0 (d, *J* = 4.0 Hz), 70.7 (br), 48.6 (d, *J* = 15.5 Hz), 47.7 (d, *J* = 21.0 Hz), 38.6, 36.2, 35.4, 28.6, 28.1, 17.5, 17.4; HRMS (ES$^+$) *m*/*z* found 569.1054 $[M + 2H]^{2+}$ $C_{38}H_{54}N_8O_{10}OsP_2Ru$ requires 569.1045; $C_{38}H_{52}N_8O_{10}P_2OsRu.5H_2O$ (%): calcd C 37.28 H 5.11 N 9.15 found C 37.36 H 4.82 N 9.16.

Complex 3b: **3a** (20 mg, 0.016 mmol based on **3a** obtained as its pentahydrate) was dissolved in $HCl_{(aq)}$ (1M, 2 ml). The solution colour quickly changed from yellow to orange – it was left to stand at room temperature for 48 h. The solution was subjected to centrifugation then added dropwise to 2-propanol (12 ml) and cooled at 4°C for 20 min. The precipitate was collected by centrifugation, redissolved in $HCl_{(aq)}$ (1M, 0.1 ml) and the product precipitated by the addition of 2-propanol. The solid was collected by centrifugation, redissolved in $HCl_{(aq)}$ (1M, 0.1 ml) then lyophilized to leave the desired product as an organge solid (14 mg). ^{1}H NMR (DMSO-d_6, 400 MHz): δ = 8.06 (s, 2H, 2 x N*H*), 6.02 (d, 2H, *J* = 5.0 Hz, 2 x Ar C*H*) 5.93 (m, 4H, 4 x Ar C*H*), 5.85 (d, 2H, *J* = 5.5 Hz, 2 x Ar C*H*), 4.83 (m br, 12H, PTA), 4.30 (s, 6H, PTA), 4.24 (s, 6H, PTA), 3.05 (m, 4H, -HN-CH_2-CH_2-NH-), 2.40 (m, 8H, -CH_2-CH_2-), 2.04 (s, 3H, ArCH_3), 1.91 (s, 3H, ArCH_3); ^{31}P{^{1}H} NMR (DMSO-d_6, 162 MHz): δ = -25.9, -68.6; HRMS (ES$^+$) *m*/*z* found 1101.1142 $[M + H]^+$ $C_{34}H_{53}Cl_4N_8O_2OsP_2Ru$ requires 1101.1143.

Complex 4a: The complex was synthesised following reported procedures[36] Analytical data was in accordance with this report. $C_{38}H_{52}N_8O_{10}P_2Ru_2.6H_2O$ (%): calcd C 39.58 H 5.59 N 9.72 found C 39.63 H 5.46 N 9.77.

An alternative route to obtain the $[Ru(\eta^6\text{-}3\text{-}(p\text{-tolyl})propanoic\ acid)Cl_2]_2$ intermediate within this synthetic procedure intermediate was also employed:-

[Ru(η^6-ethyl 3-(*p*-tolyl)propanoate)Cl_2]$_2$: To a mixture of 3-(4-methylcyclohexa-1,4-dien-1-yl)propanoic acid (1.34 g, 8.06 mmol) and 3-(*p*-tolyl)propionic acid (2.66 g, 16.20 mmol) was added $RuCl_3.xH_2O$ (0.862 g, 4.16 mmol, anhydrous basis) followed by ethanol (30 ml). The dark suspension was heated and maintained at reflux for 18 h then left to cool. The mixture was filtered to leave a black solid and a red/orange solution that was concentrated to a volume of 10 ml, diluted with diethyl ether (20 ml) the left to stand at 4°C. Over 72 h red crystals formed that were collected, washed with diethyl ether then dried under reduced pressure to yield the product as a red crystalline solid (734 mg, 1.01 mmol, 49 %). ^{1}H NMR ($CDCl_3$, 400 MHz): δ = 5.44 (d, 4H, *J* = 6.0 Hz, 4 x Ar C*H*), 5.32 (d, 4H, *J* = 6.0 Hz, 4 x Ar C*H*), 4.09 (q, 4H, *J* = 7.0 Hz, 2 x –OCH_2CH$_3$), 2.88 (t, 4H, *J* = 7.0 Hz, 2 x Ar-CH_2-CH_2-), 2.67 (t, 4H, *J* = 7.0 Hz, 2 x Ar-CH_2-CH_2-), 2.19 (s, 6H, ArCH_3), 1.22 (t, 6H, *J* = 7.0 Hz, 2 x –OCH$_2$CH_3); ^{13}C{^{1}H} NMR (DMSO-d_6, 100 MHz): δ = 172.5, 101.2, 99.2, 88.6, 86.5, 60.6, 33.1, 27.5, 18.5, 14.6; $C_{24}H_{32}Cl_4O_4Ru_2$ (%): calcd C 39.57 H 4.43 found C 39.52 H 4.69.

[Ru(η^6-3-(*p*-tolyl)propanoic acid)Cl_2]$_2$: [Ru(η^6-ethyl 3-(*p*-tolyl)propanoate)Cl_2]$_2$ (438 mg, 0.601 mmol) was suspended in HCl (1M, 10 ml) and heated at reflux for 4 h over which time the solid solubilised to form a red solution. The solution was dried under reduced pressure to leave the product as a red solid in quantitative yield. ^{1}H NMR (DMSO-d_6, 400 MHz): δ = 5.85 (d, 4H, *J* = 6.0 Hz, 4 x Ar C*H*), 5.77 (d, 4H, *J* = 6.0 Hz, 4 x Ar C*H*), 2.61 (s, 4H, 2 x Ar-CH_2-CH_2-), 2.07 (s, 6H, ArCH_3); ^{13}C{^{1}H} NMR (DMSO-d_6, 100 MHz): δ = 173.5, 100.6, 99.2, 88.0, 86.2, 32.9, 27.1, 18.0.

Complex 4b: **4a** (5.7 mg, 0.005 mmol based on **4a** obtained as its hexahydrate) was dissolved in $HCl_{(aq)}$ (1M, 0.1 ml). The solution colour changed (~5 min) from yellow to red – it was left to stand at room temperature for 2 h. The product was then precipitated by the addition of 2-propanol and the solid collected by centrifugation – the biphasic solid/liquid sample was left to stand at 4°C for 1 h then subjected to further centrifugation. The liquid was decanted, the solid washed with 2-propanol (1 ml) then dried under reduced pressure. HRMS (ES$^+$) *m*/*z* found 1013.0605 $[M + H]^+$ $C_{34}H_{53}Cl_4N_8O_2P_2Ru_2$ requires 1013.0594.

Complex 5a: TBTU (53 mg, 0.165 mmol) and [Os(η^6-3-(*p*-tolyl)propanoic acid)PTA(C_2O_4)] (100 mg, 0.168 mmol) were suspended in DMSO (1 ml) then DIPEA (174 µl, 0.999 mmol) was added and the mixture was left to stir for 5 min. Methylamine hydrochloride (11 mg, 0.163 mmol) was then added and the reaction mixture was left to stir. After 2 h the yellow solution that had formed was diluted with acetone (13 ml) to yield a precipitate – the mixture was shaken then left to settle and the solvent decanted. This process was repeated twice more then a suspension of the complex in acetone (10 ml) was added to a silica gel column (4 cm x 25 cm loaded in acetone) with acetone (20 ml) in excess in the solvent reservoir. The solvent was eluted to allow the yellow suspension to settle onto the silica gel. The column was then eluted with acetone (100 ml to remove DMSO) then MeOH (300 ml) followed by MeOH:H_2O (400 ml, 8:2). The product eluted as a yellow solution – this was filtered then dried at 60°C under reduced pressure. The residue was dissolved in MeOH (100 ml), filtered then concentrated to 5 ml and left to vapour diffuse (48 h) with diethyl ether to yield crystalline material over 24 h. The crystals were harvested and the liquid left to vapour diffuse further to yield a second batch of crystals – these were harvested and combined with the first batch. The combined solids were dissolved in H_2O (2 ml), diluted with acetone (10 ml) and left to vapour diffuse with acetone to yield crystalline material. This was harvested, dissolved in H_2O and lyophilised to remove residual solvent and leave the product as an orange yellow solid (25 mg, 0.041 mmol, 25 %). ^{1}H NMR (D_2O, 400 MHz): δ = 6.05 (d, 2H, 2H, *J* = 6.5 Hz, 2 x Ar C*H*), 6.00 (d, 2H, *J* = 6.0 Hz, 2 x Ar C*H*), 4.45-4.55 (m, 6H, PTA), 4.07 (s, 6H, PTA), 2.62 (s, 3H, -NHCH_3), 2.54 (m, 4H, -CH_2-CH_2-), 2.12 (s, 3H, ArCH_3); ^{31}P{^{1}H} NMR (D_2O, 162 MHz): δ = -66.7; ^{13}C{^{1}H} NMR (D_2O, 100 MHz): δ = 174.8, 166.0, 90.7, 87.4, 80.9 (d, *J* = 3.0 Hz), 79.9 (d, *J* = 4.0 Hz), 70.6 (d, *J* = 6.5 Hz), 47.6 (d, *J* = 21.0 Hz), 36.2, 28.8, 25.8, 17.4; HRMS (ES$^+$) *m*/*z* found 615.1423 $[M + H]^+$ $C_{19}H_{28}N_4O_5OsP$ requires 615.1407; $C_{19}H_{27}N_4O_5POs•H_2O$ (%): calcd C 36.19 H 4.64 N 8.88 found C 36.03 H 4.38 N 8.59.

Complex 5b: **5a** (4.0 mg, 0.006 mmol based on **5a** obtained as its monohydrate) was dissolved in $HCl_{(aq)}$ (1 M, 1 ml) and left to stand for 2 h. The solution was then dried under reduced pressure, dissolved in MeOH (1 ml) then the complex precipitated by the addition of diethyl ether (10 ml). The solid was isolated by centrifugation then dried under reduced pressure. HRMS (ES$^+$) *m*/*z* found 597.0987 $[M + H]^+$ $C_{17}H_{28}Cl_2N_4OOsP$ requires 597.0967.

Complex 6b: **6a** (4.0 mg, 0.008 mmol based on **6a** obtained as its hemihydrate) was dissolved in $HCl_{(aq)}$ (1 M, 1 ml) and left to stand for 2 h. The solution was then dried under reduced pressure, dissolved in MeOH (1 ml) then the complex precipitated by the addition of diethyl ether (10 ml). The solid was isolated by centrifugation then dried under reduced pressure. HRMS (ES$^+$) *m*/*z* found 507.0425 $[M + H]^+$ $C_{17}H_{28}Cl_2N_4ORuP$ requires 507.0414.

***N*,*N*'-(ethane-1,2-diyl)bis(3-(*p*-tolyl)propanamide) (7):** 3-(*p*-tolyl)propanoic acid (1 g, 6.09 mmol) was suspended in DMF (10 ml) followed by the addition of DIPEA (4.2 ml, 24.1 mmol) then TBTU (2.15 g, 6.7 mmol). The solution was stirred for 5 min followed by the addition of ethylenediamine (204 µl, 3.05 mmol) to yield an immediate precipitate. The suspension was stirred for 3 h then diluted with EtOAc (100 ml) and extracted with HCl (1M, 2 x 50 ml) then H_2O (50 ml). The organic fraction was evaporated under reduced pressure to yield a white solid that was recrystallised from DCM (100

ml) and MeOH (4 ml). The precipitated product was collected by filtration then dried under reduced pressure to leave a white solid (110 mg, 0.312 mmol, 10 %).
^{1}H NMR (DMSO-d_6, 400 MHz): δ = 7.82 (s, 2H, 2 x N*H*), 7.06 (s, 8H, Ar C*H*), 3.04 (m, 4H, 3.04, en CH_2), 2.75 (t, 4H, J = 8.0 Hz, 2 x Ar-CH_2-CH$_2$-), 2.31 (t, 4H, J = 8.0 Hz, 2 x Ar-CH$_2$-CH_2-), 2.24 (s, 6H, 2 x ArCH_3); ^{13}C{^{1}H} NMR (DMSO-d_6, 100 MHz): δ = 171.5, 138.2, 134.7, 128.8, 128.0, 38.3, 37.2, 30.6, 20.6; MS (ES$^+$) *m/z* found 353.27 [M + H]$^+$; $C_{22}H_{28}N_2O_2$ (%): calcd C 74.97 H 8.01 N 7.95 found C 74.75 H 8.18 N 7.72.

NMR stability and reactivity studies
Stability studies of complexes **2a**-**4a** were performed in D_2O (0.1 M NaCl) and McCoys 5A Medium (Modified) (supplemented with 10% fetal calf serum). The solutions of the complex were incubated at 310 K for up to 72 h and monitored by ^{1}H and/or ^{31}P{^{1}H} NMR.
The reactivity of **2b**-**4b** towards guanosine 5′-monophosphate was assessed by the incubation of the complex (3.6 mM) in a solution of guanosine 5′-monophosphate (21.6 mM, 5 mM NaCl, pD 7.4 150 mM phosphate buffer) for 72 h at 310 K and monitoring the reaction by ^{1}H NMR.

Cell culture
Protocol for cell viability experiments with HT-29 cells and **2a**-**6a**, **7** and **cisplatin**.

Preparation of the stock solutions:
2a-**6a**, **7** and **cisplatin** were weighed into glass vials. Each ruthenium/osmium complex was diluted in 1 ml of H_2O and the solutions were vortexed then filtered through a 0.22 µm syringe filter to sterilise them. Ligand **7** and **cisplatin** were first diluted into H_2O (1 ml) then DMSO (1 ml) was added followed by vortexing, sonicating and filtering as above.

Cytotoxicity experiments:
HT-29 (human colon adenocarcinoma) cells were counted and the concentration adjusted to 3 x 10^4 cells/ml. 100 µl of the cell suspension was dispensed into the wells of a 96 well plate. The cells were left to attach for 24 hours after which the original medium was removed and 100 µl of the dilutions of **2a**–**6a**, **7** or **cisplatin** (or new medium for cells only control) was added. The plates were incubated at 37°C and 5% CO_2 for 72 hours. After this incubation period 10µl of MTT solution (3-[4, 5-dimethylthiazol-2-yl]-2, 5-diphenyltetrazolium bromide - Thiazolyl blue; Sigma M5655 made up in PBS and filtered through a 0.22 µm syringe filter) was added to each well. The colour was allowed to develop for 3 hours after which the reaction was halted by adding 150µl of acid-alcohol (0.04 M HCl in isopropanol) to each well. The results were read on a plate reader (Biotek ELX800 Universal Microplate Reader) at 570 nm. The viability of the cells is expressed as % of cell survival of each dilution against the “cells only” control taken as 100 % survival.

Protocol for FACS analysis.
Cell cycle analysis was performed by flow cytometry according to the method of Nicoletti et. al.[46]

HT-29 cells with a confluence of 60-70%, were seeded onto 6-well plates (Greiner Bio-one; multiwell 6), 1.5 ml of a 1x10^5 cells/ml suspension in McCoy’s 5A modified medium supplemented with 1% L-glutamine and 10% fetal calf serum (Life Science Productions) and incubated to adhere to the plates for 24 hr at 37ºC in a 5% CO_2 humidified environment. The cells were treated with the IC_{50} concentration of complexes. At t=48 hr the cells were rinsed with 2 ml of 0.01 M PBS (Glibco®; PBS tablets). The cells were trypsinised (1 ml) at 37 ºC for ~ 5 mins. The detached cells were collected in cold media (1 ml). The floating cells and retained PBS washings were combined and centrifuged for 5 min at 1250 RPM (260 g). The supernatant was decanted and the cell pellet re-suspended into ice-cold PBS (1 ml) and transferred into FACS (Falcon) tubes and kept on ice then centrifuged as above. The supernatant was decanted and re-suspended by slowly adding ice-cold 80% EtOH (4 ml) (Honeywell; puris >99.7% GC) to each tube while vortexing, the tubes were frozen for 1 hr. Pre-prepared PI-RNaseA (Sigma-Aldrich) in PBS mixture (5x10^{-6} g/ml and 10x10^{-6} g/ml) was added. The cells were centrifuged at 1250 RPM (260 g) for 10 minutes. The supernatant was decanted and washed with ice-cold PBS (1 ml). Centrifuged again as above and re-suspend into 1 ml PI-RNasA PBS mix; incubated at room temperature and in the dark for 1 hour then transferred to ice for FACS analyses using a BD FACSCalibur Flow Cytometer (BD Biosciences) with 10,000 events being measured per plot.
FACS experiments were carried out in triplicate (n=3). Representative data are presented as forward scatter vs side scatter dot plots (Figure S8) and histograms (Figure S9). Dot plots were gated to remove multinuclear events and particle debris. Collated data were plotted on GraphPad Prism 7.0, the data are presented as the mean values, error bars are presented as standard deviations (X±SD) of three independent plated experiments performed in triplicate (n=3). Two-way multiple comparison ANOVA with Dunnett’s *post-hoc* statistical testing was carried out on represented by Figure 4. One-way ANOVA with Dunnett’s *post-hoc* statistical testing was carried out on data represented by Figure S10.

Acknowledgements

We thank the EPSRC UK National Crystallography Service at the University of Southampton for the collection of some of the crystallographic data.[47]

Conflicts of interest

The authors declare no conflict of interest.

Keywords: bioorganometallic • metallodrugs • bioinorganic • cancer • dinuclear complexes

[1] T. C. Johnstone, K. Suntharalingam, S. J. Lippard, *Chem. Rev.*, **2016**, *116*, 3436-3486.
[2] M. Allison, D. Wilson, C. M. Pask, P. C. McGowan, R. M. Lord, *ChemBioChem*, **2020**, https://doi.org/10.1002/cbic.202000028.
[3] P. Robin, K. Singh, K. Suntharalingam, *Chem. Comm.*, **2020**, *56*, 1509-1512.
[4] S. J. Allison, M. Sadiq, E. Baronou, P. A. Cooper, C. Dunnill, N. T. Georgopoulos, A. Latif, S. Shepherd, S. D. Shnyder, I. J. Stratford, R. T. Wheelhouse, C. E. Willans, R. M. Phillips, *Cancer Lett.*, **2017**, *403*, 98-107.
[5] A. P. King, S. C. Marker, R. V. Swanda, J. J. Woods, S-B. Qian, J. J. Wilson, *Chem. Eur. J.*, **2019**, *25*, 9206-9210
[6] J. P. C. Coverdale, I. Romero-Canelón, C. Sanchez-Cano, G. J. Clarkson, A. Habtemariam, M. Wills, P. J. Sadler, *Nat. Chem.*, **2018**, *10*, 347-354.
[7] H. Huang, S. Banerjee, K. Qiu, P. Zhang, O. Blacque, T. Malcomson, M. J. Paterson, G. J. Clarkson, M. Staniforth, V. G. Stavros, G. Gasser, H. Chao, P. J. Sadler, *Nat. Chem.*, **2019**, *11*, 1041–1048.
[8] a) W. Ma, L. Guo, Z. Tian, S. Zhang, X. He, J.J. Li, Y. Yang, Z. Liu, *Dalton Trans.*, **2019**, *48*, 4788-4893; b) J.J. Li, Z. Tian, X. Ge, Z. Xu, Y. Feng, Z. Liu, *Eur. J. Med. Chem.*, **2019**, *163*, 830-839.
[9] R. McCall, M. Miles, P. Lascuna, B. Burney, Z. Patel, K. J. Sidoran, V. Sittaramane, J. Kocerha, D. A. Grossie, J. L. Sessler, K. Arumugam, J. F. Arambula, *Chem. Sci.*, **2017**, *8*, 5918-5929.
[10] S. Leijen, S. A. Burgers, P. Baas, D. Pluim, M. Tibben, E. van Werkhoven, E. Alessio, G. Sava, J. H. Beijnen, J. H. M. Schellens, *Invest. New Drugs*, **2015**, *33*, 201-214.

[11] R. Trondl, P. Heffeter, C. R. Kowol, M. A. Jakupec, W. Berger, B.K. Keppler, *Chem. Sci.*, **2014**, *5*, 2925-2932.
[12] B. S. Murray, M. V. Babak, C. G. Hartinger, P. J. Dyson, *Coord. Chem. Rev.*, **2016**, *306*, 86-114.
[13] A. Habtemariam, M. Melchart, R. Fernández, S. Parsons, I. D. H. Oswald, A. Parkin, F. P. A. Fabbiani, J. E. Davidson, A. Dawson, R. E. Aird, D. I. Jodrell, P. J. Sadler, *J. Med. Chem.*, **2006**, *49*, 6858-6868.
[14] A. K. Renfrew, J. Karges, R. Scopelliti, F. D. Bobbink, P. Nowak-Sliwinska, G. Gasser, P. Dyson, *ChemBioChem*, **2019**, *20*, 2876-2882.
[15] F. Chen, I. Romero-Canelón, J. J. Soldevila-Barreda, J-I. Song, J. P. C. Coverdale, G. J. Clarkson, J. Kasparkova, A. Habtemariam, M. Wills, V. Brabec, P. J. Sadler, *Organometallics*, **2018**, *37*, 1555-1566.
[16] F. Martínez-Peña, A. M. Pizarro, *Chem. Eur. J.*, **2017**, *23*, 16231−16241.
[17] T. J. Prior, H. Savoie, R. W. Boyle, B. S, Murray, *Organometallics*, **2018**, *37*, 294−297.
[18] S. A. Kemp, T. J. Prior, H. Savoie, R. W. Boyle, B. S. Murray, *Molecules*, **2020**, *25*, 244.
[19] S. M. Meier, D. Kreutz, L. Winter, M. H. M. Klose, K. Cseh, T. Weiss, A. Bileck, B. Alte, J. C. Mader, S. Jana, A. Chatterjee, A. Bhattacharyya, M. Hejl, M. A. Jakupec, P. Heffeter, W. Berger, C. G. Hartinger, B. K. Keppler, G. Wiche, C. Gerner, *Angew. Chem. Int. Ed.*, **2017**, *56*, 8267–8271.
[20] a) R. A. Ruhayel, J. J. Moniodis, X. Yang, J. Kasparkova, V. Brabec, S. J. Berners-Price, N. P. Farrell, *Chem. Eur. J.*, **2009**, *15*, 9365 – 9374; b) J. Kasparkova, J. Zehnulova, N. Farrell, V. Brabec, *J. Biol. Chem.*, **2002**, *277*, 48076-48086.
[21] a) N. P. Farrell, *Metal Ions Biol. Syst.,*. **2004**, *41*, 252−296; b) C. Billecke, S. Finniss, L. Tahash, C. Miller, T. Mikkelsen, N. P. Farrell, O. Bogler, *Neuro-oncol.*, **2006**, *8(3)*, 215-226.
[22] J. B. Mangrum, B. J. Engelmann, E. J. Peterson, J. J. Ryan, S. J. Berners-Price, N. P. Farrell, *Chem. Commun.*, **2014**, *50*, 4056--4058
[23] E. J. Peterson, A. G. Daniel, S. J. Katner, L. Bohlmann, C.-W. Chang, A. Bezos, C. R. Parish, M. von Itzstein, S. J. Berners-Price, N. P. Farrell, *Chem. Sci.*, **2017**, *8*, 241-252
[24] A. Kumar Gorle, S. J. Katner, W. E. Johnson, D. E. Lee, A. G. Daniel, E. P. Ginsburg, M. von Itzstein, S. J. Berners-Price, N. P. Farrell, *Chem. Eur. J.*, **2018**, *24*, 6606-6616.
[25] a) M. G. Mendoza-Ferri , C. G. Hartinger , M. A. Mendoza , M. Groessl , A. E. Egger , R. E. Eichinger , J. B. Mangrum , N. P. Farrell , M. Maruszak , P. J. Bednarski , F. Klein , M. A. Jakupec , A. A. Nazarov , K. Severin and B. K. Keppler, *J. Med. Chem.*, **2009**, *52* , 916-925; b) O. Nováková , A. A. Nazarov , C. G. Hartinger , B. K. Keppler, V. Brabec, *Biochem. Pharmacol.*, **2009**, *77*, 364-374.
[26] S. Parveen, M. Hanif, E. Leung, K. K. H. Tong, A. Yang, J. Astin, G. H. De Zoysa, T. R. Steel, D. Goodman, S. Movassaghi, T. Söhnel, V. Sarojini, S. M. F. Jamieson, C. G. Hartinger, *Chem. Comm.*, **2019**, *55*, 12016-12019.
[27] L. K. Batchelor, E. Paunescu, M. Soudani, R. Scopelliti, P. J. Dyson, *Inorg. Chem.*, **2017**, *56*, 9617−9633.
[28] L. K. Batchelor, D. Ortiz, P. J. Dyson, *Inorg. Chem.*, **2019**, *58*, 2501−2513.
[29] B. Bertrand, A. Citta, I. L. Franken, M. Picquet, A. Folda, V. Scalcon, M. P. Rigobello, P. Le Gendre, A. Casini, E. Bodio, *J. Biol. Inorg. Chem.*, **2015**, *20*, 1005-1020.
[30] N. Curado, N. Giménez, K. Miachin, M. Aliaga-Lavrijsen, M. A. Cornejo, A. A. Jarzecki, M. Contel, *ChemMedChem*, **2019**, *14*, 1086-1095.
[31] B. T. Elie, Y. Pechenyy, F. Uddin, M. Contel, *J. Biol. Inorg. Chem.*, **2018**, *23*, 399-411.
[32] M. Wenzel, A. de Almeida, E. Bigaeva, P. Kavanagh, M. Picquet, P. Le Gendre, E. Bodio, A. Casini, *Inorg. Chem.*, **2016**, *55*, 2544-2557.
[33] B. T. Elie, J. Fernández-Gallardo, N. Curado, M. A. Cornejo, J. W. Ramos, M. Contel, E. *J. Med. Chem.*, **2019**, *161*, 310-322.
[34] X. Ge, S. Chen, X. Liu, Q. Wang, L. Gao, C. Zhao, L. Zhang, M. Shao, X.-A. Yuan, L. Tian, Z. Liu, *Inorg. Chem.*, **2019**, *58*, 14175-14184.
[35] L. Ma, R. Ma, Z. Wang, S.-M. Yiu, G. Zhu, *Chem. Commun.*, **2016**, *52*, 10735-10738.
[36] B. S. Murray, L. Menin, R. Scopelliti, P. J. Dyson, *Chem. Sci.*, **2014**, *5*, 2536-2545.
[37] G. E. Davey, Z. Adhireksan, Z. Ma, T. Riedel, D. Sharma, S. Padavattan, D. Rhodes, A. Ludwig, S. Sandin, B. S. Murray, P. J. Dyson, C. A. Davey, *Nat. Commun.*, **2017**, *8*, 1575.
[38] B. Wu, M. S. Ong, M. Groessl, Z. Adhireksan, C. G. Hartinger, P. J. Dyson, C. A. Davey, *Chem. Eur. J.*, **2011**, *17*, 3562-3566.
[39] A. Dorcier, P. J. Dyson, C. Gossens, U. Rothlisberger, R. Scopelliti, I. Tavernelli *Organometallics*, **2005**, *24*, 2114-2123.
[40] G.M. Sheldrick, *Acta Cryst.,* **2015**, *A71*, 3-8.
[41] G.M. Sheldrick, *Acta Cryst.,* **2015**, C**71**, 3-8.
[42] W. H. Ang, E. Daldini, C. Scolaro, R. Scopelliti, L. Juillerat-Jeannerat, P. J. Dyson, *Inorg. Chem.*, **2006**, *45*, 9006-9013.
[43] X. Elduque, E. Pedroso, A. Grandas, *J. Org. Chem.*, **2014**, *79*, 2843-2853.
[44] J. Sandland, H. Savoie, R. W. Boyle, B. S. Murray, *Inorg. Chem.*, **2020**, https://doi.org/10.1021/acs.inorgchem.0c01044.
[45] F. K. Cheung, A. M. Hayes, J. Hannedouche, A. S. Y. Yim, M. Wills, *J. Org. Chem.*, **2005**, *70*, 3188-3197.
[46] C. Riccardi, I. Nicoletti, *Nat. Protoc.,* **2006**, *1*, 1458-1461.
[47] S. J. Coles, P. A. Gale, *Chem. Sci.,* **2012**, *3*, 683-689.